RAPID COMMUNICATIONS

PHYSICAL REVIEW B VOLUME 45, NUMBER 13 1 APRIL 1992-I

Early stages of $YBa_2Cu_3O_{7-\delta}$ epitaxial growth on MgO and $SrTiO_3$

Xiang-Yang Zheng
Department of Physics and Astronomy, The University of Tennessee, Knoxville, Tennessee 37996

Douglas H. Lowndes
Solid State Division, Oak Ridge National Laboratory, Oak Ridge, Tennessee 37831-6056

Shen Zhu
Department of Physics and Astronomy, The University of Tennessee, Knoxville, Tennessee 37996

J. D. Budai
Solid State Division, Oak Ridge National Laboratory, Oak Ridge, Tennessee 37831-6024

R. J. Warmack
Health and Safety Research Division, Oak Ridge National Laboratory, Oak Ridge, Tennessee 37831-6123
(Received 26 December 1991)

The initial stages of epitaxial growth of c-axis-perpendicular laser-ablated $YBa_2Cu_3O_{7-\delta}$ (YBCO) thin films on $SrTiO_3$ and MgO substrates were studied by scanning tunneling microscopy. Surface images of films grown on $SrTiO_3$ with a sequential thickness variation reveal a transition from layerlike to island growth between 8 and 16 unit cells thickness, i.e., YBCO grows on $SrTiO_3$ by a Stranski-Krastanov mechanism. Evidence also points to the existence of a slightly larger critical thickness for the introduction of screw dislocations into those films. In contrast, even the thinnest ($\sim$8 cell thick) YBCO films were found to grow on MgO by an island mechanism, with screw-growth features clearly present.

High-quality epitaxial $YBa_2Cu_3O_{7-\delta}$ (YBCO) thin films can be obtained by several growth techniques, including pulsed-laser ablation and single- or multiple-target sputtering. These films have good superconducting properties, including a high critical current density J_c of several MA/cm^2 at 77 K ($H=0$). The vortex pinning centers responsible for the high J_c are believed to be related to crystal defects in the films, since bulk YBCO single crystals have much lower J_c, but the defects responsible for high J_c in films have not been identified. Thus, studies of the initial growth mechanism and of the formation and evolution of dislocations and other defects could provide useful information, leading to the identification of the vortex pinning centers. Such knowledge may ultimately enable us to either eliminate or introduce the relevant defects in a controlled way for different applications.

Epitaxial growth is understood to take place in three basic modes:[1] layer-by-layer (Frank–van der Merwe mode), island formation (Volmer-Weber mode), and layer-by-layer followed by island growth (Stranski-Krastanov mode). Both island and layer-by-layer growth modes of YBCO films have been reported in the literature.[2,3] Norton and Carter[2] have used transmission electron microscopy to study the initial stages of YBCO film growth on $SrTiO_3$ and MgO substrates; they found that YBCO grows by an island mechanism. However, Terashima *et al.*[3] studied the growth of YBCO films on (100) $SrTiO_3$ using reflection high-energy electron diffraction (RHEED); they interpreted the observed RHEED oscillations as being due to the layer-by-layer growth mechanism of YBCO films.

Recently, scanning tunneling microscopy (STM) has been used to study the surface morphology of YBCO films. Hawley *et al.*,[4] and Gerber *et al.*,[5] observed a high density of spiral growth structures, each of which has a screw dislocation at its center. Their findings indicate that c-axis-perpendicular ($c_\perp$) YBCO films grow as three-dimensional islands on both $SrTiO_3$ and MgO substrates, by adding material to the a-c or b-c faces of a continuous, spirally rising step. However, their studies were based mostly on thick films; no evidence was given for island *nucleation* for very thin films. They suggested that the screw dislocation growth might be an intrinsic property of sputtered high-T_c films,[5] and could be responsible for at least part of their flux pinning. However, an investigation by Norton *et al.*[6] of the growth-temperature dependence of the screw dislocation density in YBCO films suggests that the screw dislocations alone cannot account for the flux pinning. In particular, Norton *et al.* found a reduced screw dislocation density in films with the highest J_c, (i.e., those grown at relatively high temperatures).[6] Furthermore, STM studies by Schlom *et al.*,[7] and by Lowndes *et al.*[8] show that the spiral growth structures can be eliminated by using slightly (1°–3°) miscut substrates; in this case, growth nucleated at the faces of surface steps apparently is favored over screw dislocation-mediated growth. Thus, films grown on miscut substrates may provide some very important clues for the identification of high-J_c pinning centers.[8]

In this paper we report STM studies of the initial stages

of epitaxial growth for thin YBCO films of varying thickness on (001) $SrTiO_3$ and MgO substrates. Films grown on MgO substrates clearly grow by an island mechanism even at very small film thickness (nominally 8 $c_\perp$ unit cells, ~9.4 nm). In contrast, films of the same thickness grown on $SrTiO_3$ substrates have a smooth, planar appearance, indicative of a layer-by-layer growth mechanism. However, island formation was observed for thicker films grown on $SrTiO_3$, beginning at about 16 unit cells thickness (~19 nm). Thus, the STM evidence indicates that YBCO films grow on $SrTiO_3$ substrates in the Stranski-Krastanov mode. Screw growth features are present in the 8-cell-thick YBCO films on MgO substrates; however, films of the same thickness on $SrTiO_3$ substrates show no sign of screw dislocations. The screw dislocations begin to emerge in films grown on $SrTiO_3$ at a film thickness of 32 unit cells or more. This indicates that there is a critical thickness for the introduction of most of the screw dislocations in films grown on $SrTiO_3$; they may form in order to relieve strain due to film-substrate lattice-constant mismatch, or due to island coalescence.

YBCO films were grown on (001) $SrTiO_3$ and MgO substrates by pulsed KrF (248 nm) excimer laser ablation of bulk YBCO targets in 200-mTorr oxygen pressure at a heater temperature of 720 °C. The substrate surface temperature is estimated to be about 50 °C cooler. The oxygen pressure was increased immediately after deposition and the films were cooled to room temperature at 10 °C/min in ~400 Torr oxygen. The deposition rate was ~0.05 nm per laser pulse and the laser was operated at a pulse rate of 1–3 Hz. X-ray-diffraction (XRD) measurements show that YBCO films deposited under these conditions on (001)-oriented ceramic substrates grow with the c-axis perpendicular ($c_\perp$) to the substrate.

One important difference between $SrTiO_3$ and MgO, for studies of YBCO epitaxy, is that they provide quite different in-plane lattice matching with YBCO. As shown in Table I, YBCO's a-b plane lattice mismatch is only ~1% for $SrTiO_3$ but is ~9% for MgO. Previous studies have shown that YBCO grows epitaxially on (001) $SrTiO_3$ with the film and substrate ⟨110⟩ axes aligned.[9] On (001) MgO, there are a variety of in-plane orientations that have relatively low interfacial energy (calculated by near-coincidence-site lattice theory),[10,11] and many of these have been observed.[11,12] However, by using annealed MgO substrates these can be reduced to a single dominant orientation, in which the ⟨100⟩ axes of the YBCO film and MgO substrate are aligned.[12] Although this is not expected to be one of the low-energy orientations, it has been suggested that it is selected as a result of graphoepitaxial nucleation and alignment of the YBCO film by ⟨100⟩ steps on the annealed MgO surface.[2]

TABLE I. Lattice constants for YBCO, $SrTiO_3$, and MgO.

	Lattice constant (Å)				
	Room temperature			730 °C	
Material	a	b	c	a	c
$YBa_2Cu_3O_{7-\delta}$	3.819	3.886	11.680	3.896	11.97
$SrTiO_3$	3.905			3.935	
MgO	4.213			~4.253	

Samples of nominal thickness 8, 16, 32, 64, and 170 $c_\perp$ unit cells were prepared. For each film thickness, the (001) $SrTiO_3$ and MgO substrates were placed side by side and run as a batch. The samples were stored in a desiccator, and were imaged with a Nanoscope II STM in air, within a few days of preparation. A tunneling current of 200–300 pA and a voltage of 500 mV were used for imaging. The images presented here are raw data or median filtered to remove high-frequency noise. Different regions of each sample were studied, to be sure the results are representative; the images shown are typical of numerous such measurements.

Images of 8-cell-thick films on MgO substrates show a high density of islands, as shown in Fig. 1 (top). While most island sites appear to be developing screw-growth features, a few islands already have formed well-developed spirals of one-half to one turn. A side view of the images shows that the edges of many of the islands are slightly higher than their centers, indicating that the planes of growth at each YBCO island are tilted relative to the MgO substrate surface. This small tilt may be responsible for the formation of the screw dislocations; the origin of the tilt may be the large lattice mismatch between YBCO and the MgO substrate. The mismatch can be accommodated by rotation of the YBCO lattice with the rotation axis not only normal[9] to the plane of the

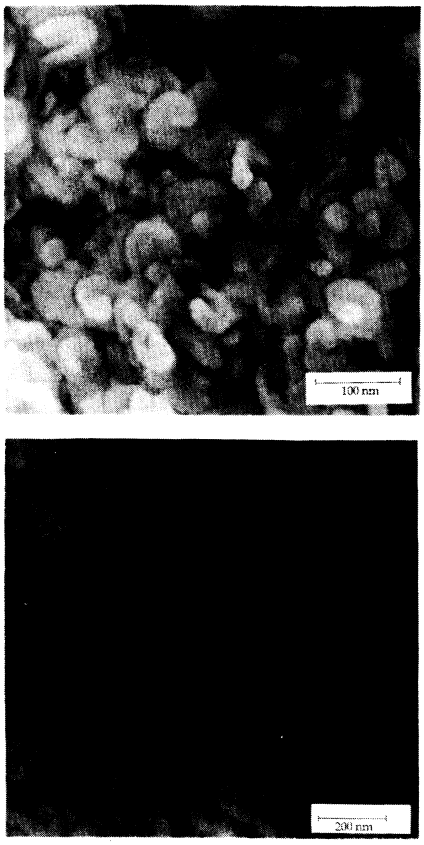

FIG. 1. STM images of $c_\perp$ YBCO films ~8 unit cells thick grown at 720 °C on (001) MgO (top) and (001) $SrTiO_3$ (bottom).

substrate-film interface but also in the plane of the interface to form tilt boundaries.[2,13,14] If the tilt planes are generated from the tilt boundaries, then the density of such boundaries should be as high as the density of the islands, and they are not unidirectional. This may be the reason why we see screw-growth features of such high density. Line-scan profiles of the STM image of Fig. 1 (top) shows that the rms surface roughness is ~1.4 nm and the largest peak-to-valley (PV) surface height variation is of the order of 6–7 nm, somewhat less than the film thickness.

The island nature of the films on MgO can be seen clearly as the film growth proceeds. Figure 2 (top) is an image from a 16-unit-cell-thick film. The boundaries between the islands become more distinct as more terraced layers are added. The diameter of each island is about 90–110 nm and the average island separation is ~130 nm. The maximum PV surface height variation is 12–17 nm and the rms surface roughness ~3.3 nm. The overlap of islands as growth proceeds results in a decrease of island density and a larger range of island sizes.

Films grown on $SrTiO_3$ display quite different features. For example, an 8-unit-cell-thick film on $SrTiO_3$ is much smoother, as shown in Fig. 1 (bottom). Line-scan profiles reveal typical PV height differences of only 2–4 nm and rms surface roughness ~1 nm, much smaller than for films of the same thickness grown on MgO [Fig. 1 (top)].

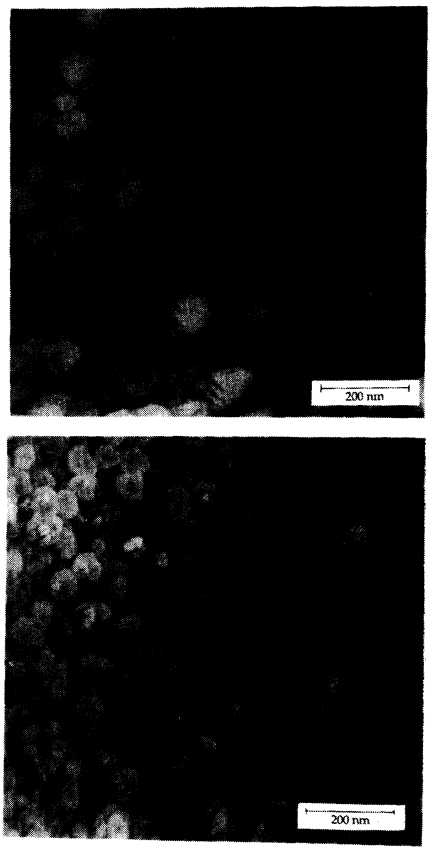

FIG. 2. STM images of $c_\perp$ YBCO films ~16 unit cells thick grown at 720 °C on (001) MgO (top) and (001) $SrTiO_3$ (bottom).

Such smoothness is consistent with growth in a layer-by-layer mode. The YBCO film grains in Fig. 1 (bottom) are asymmetric, being elongated and aligned close to the $SrTiO_3$ ⟨100⟩ axis, consistent with XRD studies of thicker films. The largest grains appear to have long dimensions ~200 nm. These features strongly suggest the two-dimensional nature of the film at this stage.

In contrast, images of 16-cell-thick YBCO films on $SrTiO_3$ clearly reveal three-dimensional island formation, as shown in Fig. 2 (bottom). Small, irregular clusters of YBCO are visible on top of nearly round, small (80–100 nm diam) YBCO plates. Histogram analysis shows that the mean height of these small plates, on top of the flat background, is 1.23 nm, about one unit cell. Line scans reveal a maximum PV surface height variation of 7–10 nm and rms roughness of 2.4 nm. This is the early stage of three-dimensional island growth, which results in islands that are stacks of terraces. No screw dislocations are seen at this early stage.

We find that screw-growth features emerge in films grown on $SrTiO_3$ when the film becomes slightly thicker. Figure 3, an image of a 32-cell-thick YBCO film on $SrTiO_3$, shows that screws of several turns are present. The layers at the spiral sites were determined by histogram analysis to have step heights of either one or two unit cells. The edges of the terraced islands again are aligned along the substrate ⟨100⟩ directions (the diagonal in Fig. 3). Line scans reveal maximum PV height variations ranging from ~4 to ~8 nm, for scans passing between or across the islands, respectively. STM images of a 64-cell-thick YBCO film grown on $SrTiO_3$ are similar to Fig. 3. Each terraced island consists of a stack of layers, and the islands have coalesced at this stage to cover the entire substrate surface. The boundaries of the islands again are aligned along the substrate ⟨100⟩ directions.

The initial growth mode of epitaxial films depends upon the relative strengths of adatom-substrate and adatom-adatom bonding, and on lattice matching.[1] If the adatom-substrate bond is strong, then layer-by-layer growth may take place initially. Otherwise, the film grows in the island mode. The large fraction of smooth film grains that are aligned with the substrate crystal lat-

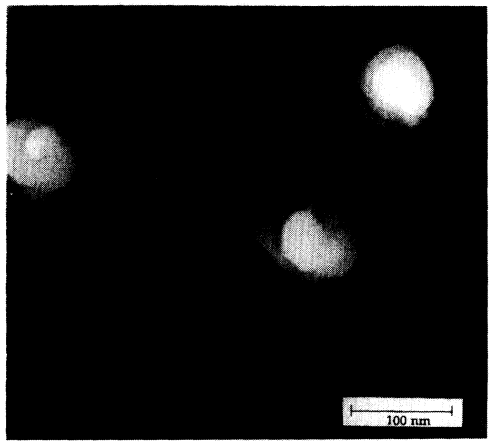

FIG. 3. STM image of $c_\perp$ YBCO film ~32 unit cells thick grown at 720 °C on (001) $SrTiO_3$.

tice in Fig. 1 (bottom) (8-cell film thickness) indicates strong bonding between the YBCO film and $SrTiO_3$ substrate. There is no obvious evidence of adatom clustering to nucleate islands at this stage; the initial nucleation and growth seems basically two dimensional. However, with increasing film thickness the added atoms (or ionic subunits) form three-dimensional islands. The switch from two-dimensional to three-dimensional growth for $SrTiO_3$ [Fig. 1 (bottom) to Fig. 2 (bottom)] is characteristic of the Stranski-Krastanov growth mode. After such a switch, the exposed *a*-*c* and *b*-*c* faces at the edges of the terraced layers of the three-dimensional YBCO islands become the rapid-growth sites. Our observations do not rule out the possibility that YBCO films grown on MgO undergo a similar change of growth mode. However, if that is the case, there may be only one or two YBCO unit cells grown on an MgO substrate when the switch to island growth occurs, due to the much larger lattice mismatch between MgO and YBCO, and we have not been able to obtain sufficiently detailed STM images for such thin films. After the switch of growth mode, films would be expected to grow in the same way on both substrates, i.e., islands become larger in size and coalesce. Indeed, there do not seem to be significant differences in the surface morphology of thick YBCO films grown on (001) $SrTiO_3$ and MgO.[4-6]

Our results are in partial agreement with the RHEED studies by Terashima *et al.*[3] of initial layer-by-layer growth of YBCO films on $SrTiO_3$. Their substrate temperature of 680 °C is close to ours of 720 °C, and their maximum film thickness of ~6 nm is well below the (8–16)-unit-cell (~9–19 nm) range in which we observe the switch from layer-by-layer growth to island growth. Ion channeling measurements of misfit strain in YBCO films grown on $SrTiO_3$, performed by Xi *et al.*,[15] also are in general agreement with our STM observations. They used inclined-direction channeling at 45° from the surface normal to show that a 9-nm-thick film was strained, but a 13-nm-thick film was not. They also found that strain was totally released in an 11-nm-thick YBCO film grown on MgO.

Our comparison of the images of films of nominal 8 unit cell thickness grown on $SrTiO_3$ and MgO (Fig. 1) demonstrates that there also is a critical thickness for introduction of screw dislocations. This critical thickness is very small for YBCO/MgO, for which the lattice misfit is ~9%. For $SrTiO_3$, with lattice misfit of ~1%, the critical thickness for the appearance of screw-growth features lies between 16 and 32 $c_\perp$ unit cells (~19–37 nm), apparently slightly thicker than for the layer-by-layer-growth to island-growth transformation. This difference in critical thicknesses for introduction of screw dislocations, for MgO and $SrTiO_3$, probably is due at least partially to the difference of lattice misfit.

There are at least two possible scenarios for the emergence of screw dislocations. As suggested by Schlom *et al.*,[7] island coalescence could lead to the generation of dislocations due to rotational, translational, or vertical misalignment of the separate islands. Since island coalescence occurs (by definition) only after the growth mode has switched from layerlike to island growth, this would explain why we do not see spiral growth features in (8–16)-unit-cell-thick films on $SrTiO_3$. Only after islands have formed and grown laterally are screw-growth features seen (Fig. 3). The island coalescence mechanism also implies that new screw dislocations can form (or terminate) throughout the growth of a thick film, so the actual density of screw-growth features in a YBCO film may not be limited to those formed near the substrate, or seen at the surface.

The other possible source of spiral-growth features (screw dislocations) is the release of strain. Strained YBCO layers, pseudomorphic to the substrate,[2] are formed at the earliest stages of epitaxial growth if the film adopts the substrate lattice parameters. As the film gets thicker, its natural lattice spacing must be restored to minimize free energy. Strain relief normally is accomplished by the introduction of dislocations near the interface, through mechanisms such as slip,[16] climb,[17] and rotation, all of which occur after a critical thickness is reached.

In summary, we have presented STM images showing that YBCO films grow on $SrTiO_3$ in the Stranski-Krastanov mode. We also find that there is a critical thickness for the introduction of screw dislocations in the YBCO films, apparently at slightly greater thickness than for the Stranski-Krastanov changeover from layerlike to island growth. The generation of a high density of screw dislocations may be due to island coalescence after the switch of the growth mode, or may be due to the release of strain caused by the lattice misfit between YBCO and the MgO or $SrTiO_3$ substrates.

This research was sponsored by the Division of Materials Sciences, U.S. Department of Energy, and by the Superconducting Technology Program for Electric Energy Systems, Advanced Utility Concepts Division, Conservation and Renewable Energy, U.S. Department of Energy, under Contract No. DE-AC05-84OR21400 with Martin Marietta Energy Systems, Inc.

[1] D. W. Pashley, Mater. Res. Soc. Symp. Proc. **37**, 67 (1985).
[2] M. Grant Norton and C. Barry Carter (unpublished).
[3] T. Terashima *et al.*, Phys. Rev. Lett. **65**, 2684 (1990).
[4] M. Hawley *et al.*, Science **251**, 1587 (1991).
[5] C. Gerber *et al.*, Nature (London) **350**, 279 (1991).
[6] D. P. Norton *et al.*, Phys. Rev. B **44**, 9760 (1991).
[7] D. G. Schlom *et al.* (unpublished).
[8] D. H. Lowndes *et al.*, in *Proceedings of Fourth International Symposium on Superconductivity, Tokyo, 1991* (Springer-Verlag, Berlin, in press); D. H. Lowndes *et al.* (unpublished).
[9] J. D. Budai *et al.*, Appl. Phys. Lett. **58**, 2174 (1991).
[10] R. W. Baluffi *et al.*, Acta Metall. **30**, 1453 (1982).
[11] D. M. Hwang *et al.*, Appl. Phys. Lett. **57**, 1690 (1990).
[12] B. H. Moeckly *et al.*, Appl. Phys. Lett. **57**, 1687 (1990).
[13] R. Du and C. P. Flynn, J. Phys. Condens. Matter **2**, 1335 (1990).
[14] B. W. Dodson *et al.*, Phys. Rev. Lett. **61**, 2681 (1988).
[15] X. X. Xi *et al.*, Appl. Phys. Lett. **54**, 2367 (1989).
[16] J. W. Matthews, Phys. Thin Films **4**, 137 (1967).
[17] K. Takayanagi *et al.*, Thin Solid Films **21**, 325 (1974).

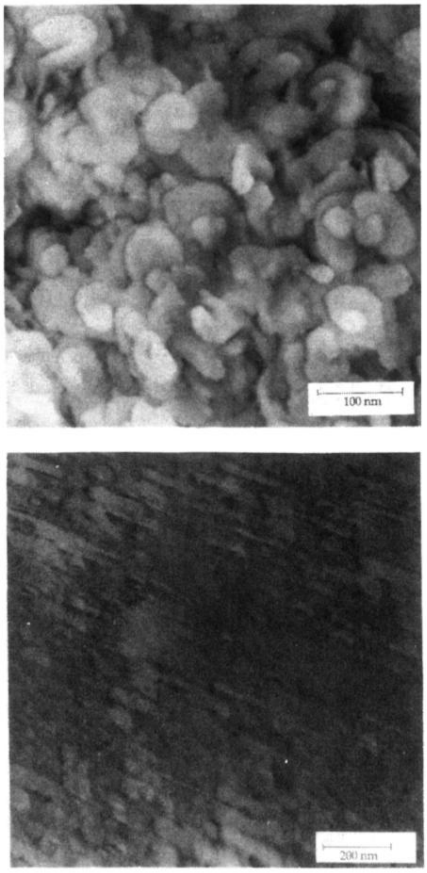

FIG. 1. STM images of $c_{\perp}$ YBCO films $\sim$8 unit cells thick grown at 720 °C on (001) MgO (top) and (001) $SrTiO_3$ (bottom).

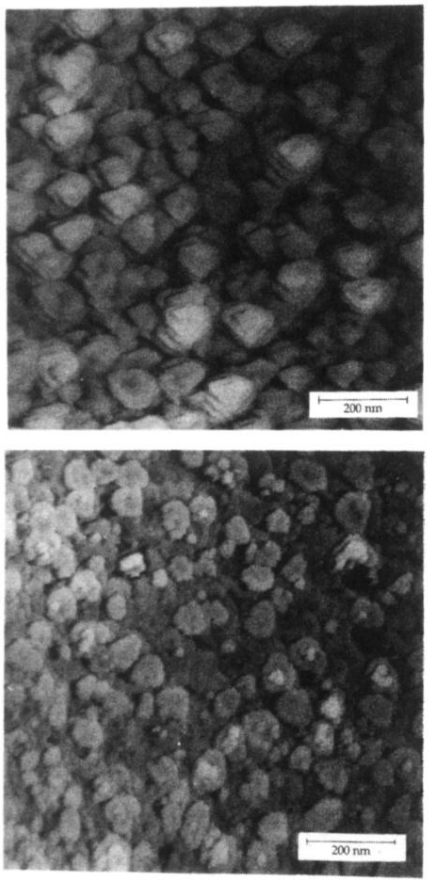

FIG. 2. STM images of $c_{\perp}$ YBCO films $\sim$16 unit cells thick grown at 720 °C on (001) MgO (top) and (001) $SrTiO_3$ (bottom).

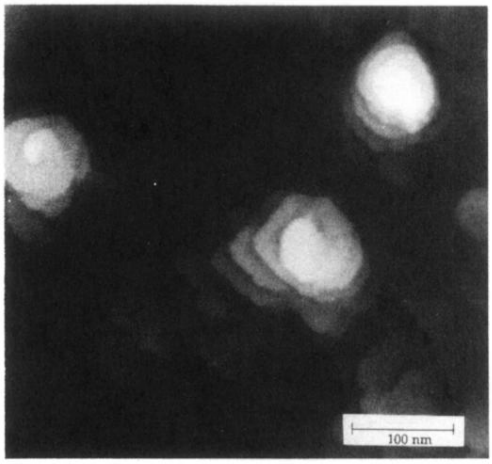

FIG. 3. STM image of $c_{\perp}$ YBCO film $\sim$32 unit cells thick grown at 720 °C on (001) $SrTiO_3$.